This article has been accepted for publication in a future issue of this journal, but has not been fully edited. Content may change prior to final publication. Citation information: DOI 10.1109/TPEL.2019.2952668, IEEE Transactions on Power Electronics

A Stator Flux Observer With Phase Self-Tuning for Direct Torque Control of Permanent Magnet Synchronous Motor

Xiaogang Lin, *Student Member*, *IEEE*, Wenxin Huang, *Member, IEEE*, Wen Jiang, *Student Member, IEEE*, Yong Zhao and Shanfeng Zhu

***Abstract*—Owing to simple implementation and excellent performance, the conventional stator flux observer based on active flux concept is considered as a competitive scheme for direct torque control (DTC) system of permanent magnet synchronous motor (PMSM). However, it is constructed by a large number of motor parameters, which may vary with the operating points. This leads to weak robustness. To improve its performance, a stator flux observer with phase self-tuning is proposed as an improved version in this paper. Firstly, relationship between the stator flux observed values obtained by current and voltage models and observed error of rotor position angle are analyzed. Then, according to the above mentioned analysis, a phase self-tuning link constructed by a proportional-integral (PI) regulator is proposed to ensure that the observed coordinate system converge to the actual one even under motor parameters vary conditions. Consequently, the robustness and accuracy of the stator flux observer can be improved. Finally, the stability of the proposed phase self-tuning link is analyzed. Experimental comparison between the conventional stator flux observer based on active flux concept and the proposed improved stator flux observer have been done, and the results verify the feasibility and effectiveness of the proposed stator flux observer.**

***Index Terms*—Direct torque control (DTC), permanent magnet synchronous motor (PMSM), stator flux observer, active flux, phase self-tuning.**

I. Introduction

With the advantages of high power density, high efficiency and simple structure, permanent magnet synchronous motor (PMSM) is widely used in industry, such as electric vehicles (EVs) and locomotive traction, *et al* [1]-[3].

As one of the control strategies for PMSM, field-oriented control (FOC) has caused wide attention since it was firstly proposed in 1970s [4]. In a FOC system, PMSM is controlled similar to a DC motor by coordinate rotation transformation and field orientation [5]. Its steady-state performance is excellent. However, the dynamic response of FOC is not rapid enough due to the inner current loop [6].

Direct torque control (DTC) is another high-performance control strategies for motor drive system. It was proposed for induction motor (IM) in 1985, and was successfully applied to PMSM in 1996 [7]. In a DTC system, the electromagnetic torque and stator flux amplitude are directly controlled by voltage vectors [8]. There is no inner current loop [9]. Hence, the dynamic response of DTC is more quick than FOC [10]. Besides, the implementation of DTC is simpler than FOC, and coordinate rotation transformation is no longer required. Therefore, DTC is a splendid choice on the high-performance drive occasions for PMSM [11], [12].

In order to obtain the superior performance for a DTC system, the stator flux observer is crucial. If the detected back electromotive force (back-EMF) is equal to the ideal value completely, the observed stator flux with high accuracy can be easily obtained by the pure integrator. This kind of stator flux observer based on the detected back-EMF is known as the voltage model. However, the output value of pure integrator would be saturated due to the unavoidable DC component in the actual analogue measurement. To overcome this problem, some improved stator flux observers based on the voltage model were proposed by researchers [13], [14]. In [13], a low pass filter with steady state error compensation was proposed to replace the pure integrator. In [14], a non-linear perpendicular stator flux observer with feedback compensation was proposed. The above stator flux observers are based on only the voltage model, which is an open-loop structure in essence. They are difficult to satisfy the strict requirements of high-performance DTC drive system.

In [15]-[24], several closed-loop stator flux observers based on both the voltage model and the current model were proposed to further improve the operation performance of DTC system. In [15], an adaptive stator flux observer was proposed for position sensorless DTC system. In [16], a sigmoid function was utilized as the switching function instead of the signum function. Then, the high frequency chattering of the conventional sliding mode observers (SMO) can be reduced. Based on the proposed SMO, the operation performance of motor drive system was improved. In [17], an adaptive full order observer was proposed to enhance the accuracy of stator flux observer, and the feedback gain of the observer is analyzed. In [18], an extended Kalman observer was utilized to observe the stator flux in a PMSM drive system. However, its computation burden is too heavy. To overcome the problem in [18], a reduced-order extended Kalman observer for PMSM is implemented by FPGA in [19].

Genarally, the performance of the closed-loop stator flux observers in [15]-[19] has been improved greatly when compared with the observers in [13] and [14]. However, the stator flux observers in [15]-[19] can be easily implemented only for a surface mounted permanent magnet synchronous motors (SPMSMs), but not for an interior permanent magnet synchronous motors (IPMSMs). This is because the

This article has been accepted for publication in a future issue of this journal, but has not been fully edited. Content may change prior to final publication. Citation information: DOI 10.1109/TPEL.2019.2952668, IEEE Transactions on Power Electronics

mathematical model of IPMSM is more complex than SPMSM.

In order to ensure that the stator flux observers can be applicable for both of the SPMSM and IPMSM, the concept of "active flux" was proposed in [20]. Based on the proposed concept, the complex part of mathematical model caused by the salient pole can be simplified in IPMSM. Then, this kind of stator flux observer for IPMSM is implemented as easily as SPMSM. In [21], the physical significance of the active flux is introduced in more detail. The defined active flux vector is always in the same direction of rotor flux vector in essence. In [22], a SMO is combined with the active flux to improve the performance of stator flux observer. In [23], the active flux concept is applied to the stator flux observer for a concentrated-wound IPMSM. In [24], by defining some modified variables, this kind of stator flux observer is extended to a six-phase PMSM with two opened phases.

Although the stator flux observers based on active flux were widely researched [20]-[24], their robustness to the motor parameters variation was not studied. As known, the motor parameters of PMSM could vary owing to magnetic saturation, cross-coupling effects and temperature variation [25]. The above stator flux observers are strongly dependent on motor parameters, such as stator resistance, stator inductance and permanent magnet flux, *et al*. If these parameters vary, the obtained observed values of stator flux may be not accurate enough. This poses a great challenge for the DTC system in real-world applications. To obtain the excellent performance of DTC for PMSM, a stator flux observer with strong robustness and high accuracy is necessary. According to the research on the conventional stator flux observer based on active flux concept, this paper proposes an improved version, which has a phase self-tuning link.

The innovations and contributions of this paper can be summarized as following three points:

1) The basic principle and the stability analysis of the conventional stator flux observer based on active flux concept is briefly introduced. On this basis, the main reasons caused weak robustness to motor parameters variation are analyzed;
2) To improve the performance, a stator flux observer with phase self-tuning is proposed. By the proposed phase self-tuning link, the observed coordinate system can converge to the actual coordinate system as soon as possible even under the motor parameters vary conditions. As a result, the robustness and accuracy of the stator flux observer is improved greatly;
3) The stability analysis of the proposed phase self-tuning link has been done. Then, the value of the proportional integral (PI) parameters in the proposed phase self-tuning link can be tuned easily.

The proposed stator flux observer and the conventional stator flux observer are compared by experimental research. The experimental results show that the proposed stator flux observer is feasible and effective. The rest of this paper is organized as follows. The mathematical model is provided in Section II. The conventional stator flux observer based on active flux concept is introduced in Section III. The introduction of the proposed stator flux observer is presented in Section IV. The experimental results are provided in Section V. Finally, some conclusions are drawn in Section VI.

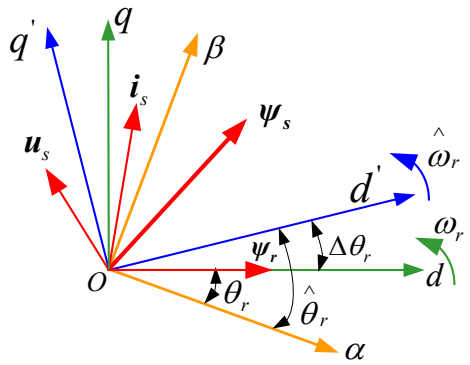

Fig. 1.Vector diagram.

II. Mathematical Model

Fig. 1 is the vector diagram. As shown, α-β axes is stator static coordinate system. d-q axes and d'-q' axes are the actual and the observed rotor synchronous coordinate system, respectively. In Fig. 1, the angle θ_r between α-axis and d-axis is the actual rotor position angle. ω_r is the rotor rotating electrical angular velocity. $\hat{\theta}_r$ and $\hat{\omega}_r$ are the observed values of θ_r and ω_r, respectively. $\Delta\theta_r$ is the observed error of θ_r.

As shown in Fig. 1, $\boldsymbol{u}_s$, $\boldsymbol{i}_s$, $\boldsymbol{\psi}_s$, $\boldsymbol{\psi}_r$ are stator voltage vector, stator current vector, stator flux vector and rotor flux vector, respectively. Their projection components on α-β axes and d-q axes are marked by subscript "α" "β" and "d" "q", respectively. The projection components of above vectors on d'-q' axes are marked by "^".

In α-β axes, the stator voltage and stator current equations can be described as shown in (1) and (2), respectively [22].

$$\begin{pmatrix} \frac{d\psi_{s\alpha}}{dt} \\ \frac{d\psi_{s\beta}}{dt} \end{pmatrix} = \begin{pmatrix} u_{s\alpha} \\ u_{s\beta} \end{pmatrix} - R_s \begin{pmatrix} i_{s\alpha} \\ i_{s\beta} \end{pmatrix} \tag{1}$$

$$\begin{pmatrix} i_{s\alpha} \\ i_{s\beta} \end{pmatrix} = \boldsymbol{T}_{\theta_r} \boldsymbol{L}^{-1} \boldsymbol{T}_{\theta_r}^{-1} \begin{pmatrix} \psi_{s\alpha} \\ \psi_{s\beta} \end{pmatrix} - \frac{\psi_f}{L_d} \begin{pmatrix} \cos\theta_r \\ \sin\theta_r \end{pmatrix} \tag{2}$$

where

$$\boldsymbol{T}_{\theta_r} = \begin{pmatrix} \cos\theta_r & -\sin\theta_r \\ \sin\theta_r & \cos\theta_r \end{pmatrix} \tag{3}$$

$$\boldsymbol{L} = \begin{pmatrix} L_d & 0 \\ 0 & L_q \end{pmatrix} \tag{4}$$

R_s is the stator resistance, L_d and L_q are respectively the d- and q-axis inductance, ψ_f is the permanent magnet flux.

In d-q axes, the stator flux can be deduced as shown in (5) [22].

$$\begin{pmatrix} \psi_{sd} \\ \psi_{sq} \end{pmatrix} = \begin{pmatrix} L_d & 0 \\ 0 & L_q \end{pmatrix} \begin{pmatrix} i_{sd} \\ i_{sq} \end{pmatrix} + \begin{pmatrix} \psi_f \\ 0 \end{pmatrix} \tag{5}$$

According to the formula (5), the stator current in d-q axes can be further deduced as shown in (6).

$$\begin{pmatrix} i_{sd} \\ i_{sq} \end{pmatrix} = \frac{1}{L_d L_q} \begin{pmatrix} L_q & 0 \\ 0 & L_d \end{pmatrix} \begin{pmatrix} \psi_{sd} \\ \psi_{sq} \end{pmatrix} - \frac{\psi_f}{L_d L_q} \begin{pmatrix} L_q \\ 0 \end{pmatrix} \tag{6}$$

This article has been accepted for publication in a future issue of this journal, but has not been fully edited. Content may change prior to final publication. Citation information: DOI 10.1109/TPEL.2019.2952668, IEEE Transactions on Power Electronics

III. Conventional Stator Flux Observer Based on Active Flux Concept Without Phase Self-Tuning

A. Basic Principle

In order to construct a closed-loop stator flux observer, both of the current model and the voltage model should be utilized. As can be seen in formula (2), the rotor position angle is necessary in the current model. Usually, the rotor position angle can be obtained by position sensor, which is in a hardware method. Or, it can be obtained by software, namely the rotor position observer. Since the system cost and reliability would be increased if additional hardware is required, the rotor position observer could be a better choice. Therefore, the rotor position observer is adopted to calculate the rotor position angle in this paper.

As shown in Fig. 1 and the formulas (1)-(6), it is not easy to obtain the rotor position angle for a IPMSM directly if only the existed variables in Fig. 1 are utilized. This is because all of the existed variables are not in the same direction with the rotor flux vector. If one variable is in the same direction with rotor flux vector, the rotor position angle can be obtained easily by solving its phase angle. Based on this idea, the active flux concept is proposed in [20]-[24]. The details are shown below.

In order to ensure that the defined variable is coincided with *d*-axis (namely the direction of the rotor flux vector), its *q*-axis component should be zero. As shown in formula (5), the *q*-axis component of stator flux is not equal to zero. To make its *q*-axis component be equal to zero, the active flux is defined in (7). Namely, the active flux vector is the stator flux vector minus the product of L_q and stator current vector.

$$\begin{pmatrix}\psi_{ad}\\ \psi_{aq}\end{pmatrix}=\begin{pmatrix}\psi_{sd}\\ \psi_{sq}\end{pmatrix}-L_q\begin{pmatrix}i_{sd}\\ i_{sq}\end{pmatrix}=\begin{pmatrix}\left(L_d-L_q\right)i_{sd}+\psi_f\\ 0\end{pmatrix} \tag{7}$$

where ψ_{ad} and ψ_{aq} are the *d*- and *q*-axes component of active flux, respectively.

According to the definition in (7), the active flux vector is coincided with *d*-axis for the reason that its *q*-axis component is zero. Therefore, the phase angle of the active flux vector is equal to the rotor position angle if the observed stator flux track the actual one well.

Generally, it is easier to get the phase angle of the defined vector in the static coordinate system than in the rotor synchronous coordinate system. Consequently, the active flux in the *d*-*q* axes shown in formula (7) is transformed to *α*-*β* axes as below:

$$\begin{pmatrix}\hat{\psi}_{a\alpha}\\ \hat{\psi}_{a\beta}\end{pmatrix}=\left(\left(L_d-L_q\right)i_{sd}+\psi_f\right)\begin{pmatrix}\cos\hat{\theta}_r\\ \sin\hat{\theta}_r\end{pmatrix}=\begin{pmatrix}\hat{\psi}_{s\alpha}\\ \hat{\psi}_{s\beta}\end{pmatrix}-L_q\begin{pmatrix}i_{s\alpha}\\ i_{s\beta}\end{pmatrix} \tag{8}$$

Based on the obtained active flux vector in formula (8), the rotor position angle can be calculated according to the following expression:

$$\hat{\theta}_r=\arctan\left(\frac{\hat{\psi}_{a\beta}}{\hat{\psi}_{a\alpha}}\right) \tag{9}$$

As known, the rotor speed is the differential of rotor position angle. Hence, the observed rotor speed $\hat{\omega}_r$ can be obtained as follows:

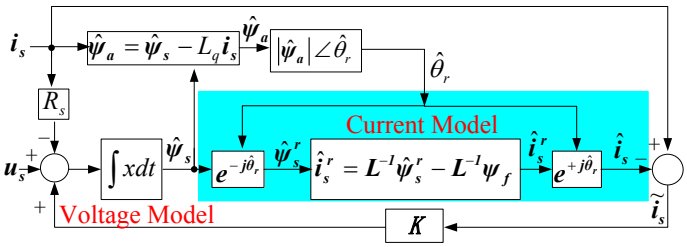

Fig. 2 The conventional stator flux observer based on active flux concept.

$$\hat{\omega}_r=\frac{d}{dt}\left(\arctan\left(\frac{\hat{\psi}_{a\beta}}{\hat{\psi}_{a\alpha}}\right)\right)=\frac{\frac{d\hat{\psi}_{a\beta}}{dt}\hat{\psi}_{a\alpha}-\frac{d\hat{\psi}_{a\alpha}}{dt}\hat{\psi}_{a\beta}}{\hat{\psi}_{a\alpha}^2+\hat{\psi}_{a\beta}^2} \tag{10}$$

According to the above deduction, the rotor position angle, which is necessary in the current model, can be obtained. On this basis, the closed-loop stator flux observer could be constructed.

Based on formulas (1)-(2) and (7)-(9), the observed voltage model and current model of stator flux are constructed as shown in (11) and (12), respectively.

$$\begin{pmatrix}\frac{d\hat{\psi}_{s\alpha}}{dt}\\ \frac{d\hat{\psi}_{s\beta}}{dt}\end{pmatrix}=\begin{pmatrix}u_{s\alpha}\\ u_{s\beta}\end{pmatrix}-R_s\begin{pmatrix}i_{s\alpha}\\ i_{s\beta}\end{pmatrix}+\boldsymbol{K}\begin{pmatrix}\tilde{i}_{s\alpha}\\ \tilde{i}_{s\beta}\end{pmatrix} \tag{11}$$

$$\begin{pmatrix}\hat{i}_{s\alpha}\\ \hat{i}_{s\beta}\end{pmatrix}=\boldsymbol{T}_{\hat{\theta}_r}\boldsymbol{L}^{-1}\boldsymbol{T}_{\hat{\theta}_r}^{-1}\begin{pmatrix}\hat{\psi}_{s\alpha}\\ \hat{\psi}_{s\beta}\end{pmatrix}-\frac{\psi_f}{L_d}\begin{pmatrix}\cos\hat{\theta}_r\\ \sin\hat{\theta}_r\end{pmatrix} \tag{12}$$

where

$$\boldsymbol{T}_{\hat{\theta}_r}=\begin{pmatrix}\cos\hat{\theta}_r & -\sin\hat{\theta}_r\\ \sin\hat{\theta}_r & \cos\hat{\theta}_r\end{pmatrix} \tag{13}$$

$$\boldsymbol{K}=\begin{pmatrix}k_{\alpha1} & k_{\beta1}\\ k_{\alpha2} & k_{\beta2}\end{pmatrix} \tag{14}$$

Remarkably, the variables marked by "~" in this paper stand for the observed errors, which are equal to the actual values minus the observed values. $\boldsymbol{K}$ is the gain coefficients of error.

According to the observed voltage model in (11) and the observed current model in (12), the closed-loop stator flux observer based on active flux concept can be constructed as shown in Fig. 2. Where, $\boldsymbol{u}_s$ and $\boldsymbol{i}_s$ are the actual voltage vector and the actual stator current vector in *α*-*β* axes, respectively. $\hat{\boldsymbol{\psi}}_s$ and $\hat{\boldsymbol{\psi}}_a$ are the observed stator flux vector and the observed active flux vector in *α*-*β* axes, respectively. $\hat{\boldsymbol{\psi}}_s^r$ and $\hat{\boldsymbol{i}}_s^r$ are the observed stator flux vector and the observed stator current vector in the *d'*-*q'* axes, respectively. $\tilde{\boldsymbol{i}}_s$ is the observed error of stator current in *α*-*β* axes.

According to the analysis above, the observed rotor speed is not necessary in the stator flux observer. However, it is essential in the speed loop. Furthermore, it is worth noting that the observer in Fig. 2 is defined as the conventional stator flux observer based on active flux without phase self-tuning, and it

This article has been accepted for publication in a future issue of this journal, but has not been fully edited. Content may change prior to final publication. Citation information: DOI 10.1109/TPEL.2019.2952668, IEEE Transactions on Power Electronics

is abbreviated as the conventional stator flux observer in the following. The proposed stator flux observer in section IV is an improved version of the conventional stator flux observer.

B. Stability Analysis

The stability analysis of the conventional stator flux is as follows. Similar to the deduction in [21] and [24], the observed error of rotor position angle is assumed to be zero. Meanwhile, the motor parameters are assumed to be matched with the actual values completely. Based on the actual current model as shown in (2) and the observed current model as shown in (12), the relationship between the observed error of stator current and the observed error of stator flux can be deduced as shown in (15).

$$\begin{pmatrix} \tilde{i}_{s\alpha} \\ \tilde{i}_{s\beta} \end{pmatrix} = \boldsymbol{T}_{\hat{\theta}_r} \boldsymbol{L}^{-1} \boldsymbol{T}^{-1}_{\hat{\theta}_r} \begin{pmatrix} \tilde{\psi}_{s\alpha} \\ \tilde{\psi}_{s\beta} \end{pmatrix} \tag{15}$$

Similarity, based on the actual voltage model as shown in (1) and the observed voltage model as shown in (11), the relationship between the observed error of stator current and the differential of observed error of stator flux can be deduced as follows.

$$\begin{pmatrix} \frac{d\tilde{\psi}_{s\alpha}}{dt} \\ \frac{d\tilde{\psi}_{s\beta}}{dt} \end{pmatrix} = -\boldsymbol{K} \begin{pmatrix} \tilde{i}_{s\alpha} \\ \tilde{i}_{s\beta} \end{pmatrix} \tag{16}$$

To analyze the stability of the conventional stator flux observer, a Lyapunov function is defined as shown in (17).

$$V = \frac{1}{2} \begin{pmatrix} \tilde{\psi}_{s\alpha} \\ \tilde{\psi}_{s\beta} \end{pmatrix}^T \boldsymbol{T}_{\hat{\theta}_r} \boldsymbol{L}^{-1} \boldsymbol{T}^{-1}_{\hat{\theta}_r} \begin{pmatrix} \tilde{\psi}_{s\alpha} \\ \tilde{\psi}_{s\beta} \end{pmatrix} > 0 \tag{17}$$

Based on the formulas in (15) and (16), the differential of (17) can be further deduced as follows:

$$\frac{dV}{dt} = -\begin{pmatrix} \tilde{i}_{s\alpha} \\ \tilde{i}_{s\beta} \end{pmatrix}^T \left(\boldsymbol{K} - \frac{1}{2} \hat{\omega}_r \left(L_q - L_d \right) T_{2\hat{\theta}_r} \right) \begin{pmatrix} \tilde{i}_{s\alpha} \\ \tilde{i}_{s\beta} \end{pmatrix} \tag{18}$$

where

$$\boldsymbol{T}_{2\hat{\theta}_r} = \begin{pmatrix} -\sin 2\hat{\theta}_r & \cos 2\hat{\theta}_r \\ \cos 2\hat{\theta}_r & \sin 2\hat{\theta}_r \end{pmatrix} \tag{19}$$

To ensure that the observed stator currents converge to the actual values, the formula (18) must be less than 0. Therefore, the following expression should be satisfied:

$$\begin{pmatrix} k_{\alpha 1} & k_{\beta 1} \\ k_{\alpha 2} & k_{\beta 2} \end{pmatrix} - \frac{1}{2} \hat{\omega}_r \left(L_q - L_d \right) \begin{pmatrix} -\sin 2\hat{\theta}_r & \cos 2\hat{\theta}_r \\ \cos 2\hat{\theta}_r & \sin 2\hat{\theta}_r \end{pmatrix} > 0 \tag{20}$$

According to the deduction as shown in (20), the system can be stable only if the error gain coefficients are shown as:

$$\begin{cases} k_{\alpha i} \left(i = 1,2 \right) > \left| \frac{1}{2} \hat{\omega}_r \left(L_q - L_d \right) \right| \\ k_{\beta i} \left(i = 1,2 \right) > \left| \frac{1}{2} \hat{\omega}_r \left(L_q - L_d \right) \right| \end{cases} \tag{21}$$

IV. Proposed Stator Flux Observer Based on Active Flux With Phase Self-Tuning

A. Problems of The Conventional Stator Flux Observer and Motivations of Proposing an Improved Version

There are several problems in the conventional stator flux observer based on active flux concept shown in Section III. They are summarized as follows:

1) The stability analysis of the conventional stator flux observer in Section III.B is based on the assumption that the observed rotor position angle is equal to the actual rotor position angle [21], [24]. However, the observed rotor position angle may not track the actual rotor position very well during the dynamic process. Hence, the range of stability of the stator flux observer is not completely correct if the above assumption is invalid;
2) Under the condition of the stator resistance variation, the observed error of stator flux obtained by the voltage model cannot be ignored. As seen in Fig. 2, the rotor position angle utilized in the current model is calculated according to the voltage model. Therefore, the observed accuracy of current model would be decreased if the voltage model of stator flux is not accurate enough. This may further worse the performance of the stator flux observer in Fig. 2;
3) The observed stator current is obtained according to the current model, which contains a large number of motor parameters, such as *d*-axis inductance, *q*-axis inductance and permanent magnet flux, *et al*. Under the condition that the measured values of these motor parameters are not completely matched with their actual values, it is impossible to observe the accurate stator flux even if the rotor position angle is completely correct.

According to the analysis above, the robustness of the conventional stator flux observer based on active flux concept is not strong enough. Furthermore, the stability analysis in Section III.B would be invalid if the observed value of rotor position angle cannot converge to their actual value as soon as possible. To overcome the disadvantages of the conventional stator flux observer, a stator flux observer with phase self-tuning is proposed as an improved version of Fig. 2.

B. Basic Principle of Proposed Stator Flux Observer

According to the coordinate definitions in Fig. 1, the variables can be transformed from *d*-*q* axes to *d′*-*q′* axes by the following transformation matrix:

$$\boldsymbol{T}_{\Delta\theta_r} = \begin{pmatrix} \cos\Delta\theta_r & \sin\Delta\theta_r \\ -\sin\Delta\theta_r & \cos\Delta\theta_r \end{pmatrix} \tag{22}$$

Therefore, the stator flux and stator current in *d′*-*q′* axes are deduced as shown in (23) and (24), respectively.

$$\begin{pmatrix} \hat{\psi}_{sd} \\ \hat{\psi}_{sq} \end{pmatrix} = \begin{pmatrix} \cos\Delta\theta_r & \sin\Delta\theta_r \\ -\sin\Delta\theta_r & \cos\Delta\theta_r \end{pmatrix} \begin{pmatrix} \psi_{sd} \\ \psi_{sq} \end{pmatrix} \tag{23}$$

$$\begin{pmatrix} \hat{i}_{sd} \\ \hat{i}_{sq} \end{pmatrix} = \begin{pmatrix} \cos\Delta\theta_r & \sin\Delta\theta_r \\ -\sin\Delta\theta_r & \cos\Delta\theta_r \end{pmatrix} \begin{pmatrix} i_{sd} \\ i_{sq} \end{pmatrix} \tag{24}$$

Substitute the actual stator flux as shown in (5) into formula (23), the stator flux in *d′*-*q′* axes can be deduced as:

This article has been accepted for publication in a future issue of this journal, but has not been fully edited. Content may change prior to final publication. Citation information: DOI 10.1109/TPEL.2019.2952668, IEEE Transactions on Power Electronics

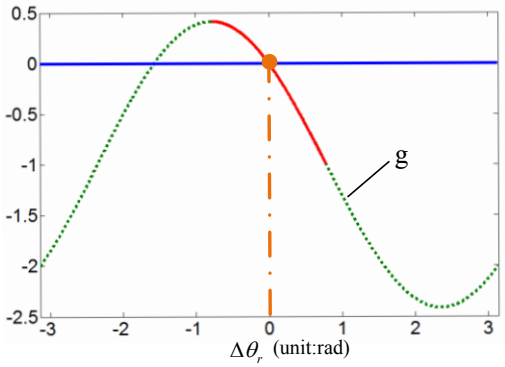

Fig. 3 The waveform of the variable *g*.

$$\begin{pmatrix} \hat{\psi}_{sd} \\ \hat{\psi}_{sq} \end{pmatrix} = \begin{pmatrix} \cos\Delta\theta_r & \sin\Delta\theta_r \\ -\sin\Delta\theta_r & \cos\Delta\theta_r \end{pmatrix} \begin{pmatrix} L_d i_{sd} + \psi_f \\ L_q i_{sq} \end{pmatrix} \tag{25}$$

According to the relationship as shown in (24), the stator current in *d*-*q* axes can be expressed by the stator current in *d*′-*q*′ axes:

$$\begin{pmatrix} i_{sd} \\ i_{sq} \end{pmatrix} = \begin{pmatrix} \cos\Delta\theta_r & -\sin\Delta\theta_r \\ \sin\Delta\theta_r & \cos\Delta\theta_r \end{pmatrix} \begin{pmatrix} \hat{i}_{sd} \\ \hat{i}_{sq} \end{pmatrix} \tag{26}$$

Substitute (26) into (25), the stator flux in *d*′-*q*′ axes can be further deduced as shown in (27) and (28).

$$\begin{aligned} \hat{\psi}_{sd} &= \left(L_d \left(\hat{i}_{sd} \cos\Delta\theta_r - \hat{i}_{sq} \sin\Delta\theta_r \right) + \psi_f \right) \cos\Delta\theta_r \\ &+ \left(L_q \left(\hat{i}_{sd} \sin\Delta\theta_r + \hat{i}_{sq} \cos\Delta\theta_r \right) \right) \sin\Delta\theta_r \end{aligned} \tag{27}$$

$$\begin{aligned} \hat{\psi}_{sq} &= -\left(L_d \left(\hat{i}_{sd} \cos\Delta\theta_r - \hat{i}_{sq} \sin\Delta\theta_r \right) + \psi_f \right) \sin\Delta\theta_r \\ &+ \left(L_q \left(\hat{i}_{sd} \sin\Delta\theta_r + \hat{i}_{sq} \cos\Delta\theta_r \right) \right) \cos\Delta\theta_r \end{aligned} \tag{28}$$

Simplify the trigonometric functions in above formulas, (27) and (28) can be further deduced as follows:

$$\begin{aligned} \hat{\psi}_{sd} &= \psi'_{sd} + \psi_f \left(\cos\Delta\theta_r - 1 \right) \\ &+ \left(L_d - L_q \right) \sin\Delta\theta_r \left(-\hat{i}_{sd} \sin\Delta\theta_r + \hat{i}_{sq} \cos\Delta\theta_r \right) \end{aligned} \tag{29}$$

$$\begin{aligned} \hat{\psi}_{sq} &= \psi'_{sq} - \psi_f \sin\Delta\theta_r \\ &+ \left(L_d - L_q \right) \sin\Delta\theta_r \left(-\hat{i}_{sd} \cos\Delta\theta_r + \hat{i}_{sq} \sin\Delta\theta_r \right) \end{aligned} \tag{30}$$

where ψ'_{sd} and ψ'_{sq} are respectively the *d*′- and *q*′-axes components of stator flux, which can be calculated according to current model. The concrete expressions of ψ'_{sd} and ψ'_{sq} are as shown in (31) and (32).

$$\psi'_{sd} = L_d \hat{i}_{sd} + \psi_f \tag{31}$$

$$\psi'_{sq} = L_q \hat{i}_{sq} \tag{32}$$

Since the observed error of rotor position angle cannot be obtained in real-world application, it is difficult to control this variable directly. In order to force the observed error of rotor position angle to be zero, a variable relevant to the observed error of rotor position angle is necessary. From this point of view, a variable *g* is defined in this paper. Its concrete expression is shown in (33).

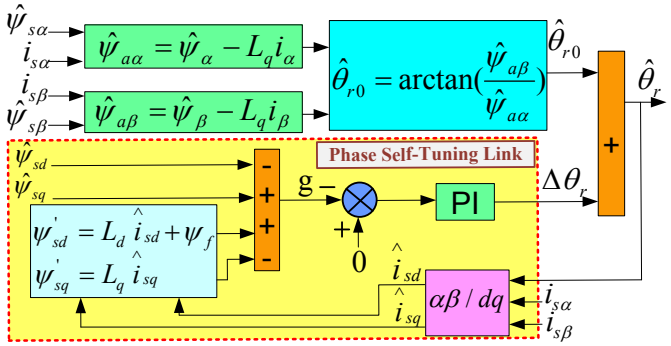

Fig. 4 The proposed phase self-tuning method.

$$\begin{aligned} g &= \left(\hat{\psi}_{sq} - \psi'_{sq} \right) - \left(\hat{\psi}_{sd} - \psi'_{sd} \right) \\ &= -\psi_f \sin\Delta\theta_r + \left(L_d - L_q \right) \sin\Delta\theta_r \left(-\hat{i}_{sd} \cos\Delta\theta_r + \hat{i}_{sq} \sin\Delta\theta_r \right) \\ &-\psi_f \left(\cos\Delta\theta_r - 1 \right) - \left(L_d - L_q \right) \sin\Delta\theta_r \left(-\hat{i}_{sd} \sin\Delta\theta_r + \hat{i}_{sq} \cos\Delta\theta_r \right) \\ &= \left(L_d - L_q \right) \sin\Delta\theta_r \left(\sin\Delta\theta_r - \cos\Delta\theta_r \right) \left(\hat{i}_{sd} + \hat{i}_{sq} \right) \\ &-\sqrt{2}\psi_f \left(\sin\left(\Delta\theta_r - \frac{\pi}{4} \right) + \frac{\sqrt{2}}{2} \right) \end{aligned} \tag{33}$$

For a SPMSM, the *d*-axis inductance is equal to the *q*-axes inductance. Thus, the expression in (33) can be simplified as:

$$g = -\sqrt{2}\psi_f \left(\sin\left(\Delta\theta_r - \frac{\pi}{4} \right) + \frac{\sqrt{2}}{2} \right) \tag{34}$$

For a IPMSM, the same expression as (34) can be also obtained under the condition that the salient pole ratio is not very large or the observed error of rotor position angle is relatively small.

According to formula (34), the waveform of the variable *g* is obtained as shown in Fig. 3. As can be seen, when $\Delta\theta_r$ falls in the region of $[-\pi/4, \pi/4]$, the defined variable *g* always has the opposite polarity with $\Delta\theta_r$. Namely, *g*<0 if $\Delta\theta_r > 0$. Conversely, *g*>0 if $\Delta\theta_r < 0$. Therefore, the polarity of $\Delta\theta_r$ can be judged easily according to the polarity of the variable *g*.

According to the analysis above, $\Delta\theta_r$ can be controlled to zero if the defined variable *g* is forced to zero. In another word, $\Delta\theta_r$ can be adjusted adaptively if the variable *g* is well controlled. Once $\Delta\theta_r$ is controlled to zero, the observed coordinate system could converge to the actual coordinate system. To achieve this goal, a phase self-tuning link based on a PI regulator is proposed in Fig. 4.

Apply the proposed phase self-tuning link in Fig. 4 to the conventional stator flux observer based on active flux concept. Thus, the proposed stator flux observer based on active flux concept with phase self-tuning can be constructed as shown in Fig. 5. As shown, the initial value of observed rotor position

This article has been accepted for publication in a future issue of this journal, but has not been fully edited. Content may change prior to final publication. Citation information: DOI 10.1109/TPEL.2019.2952668, IEEE Transactions on Power Electronics

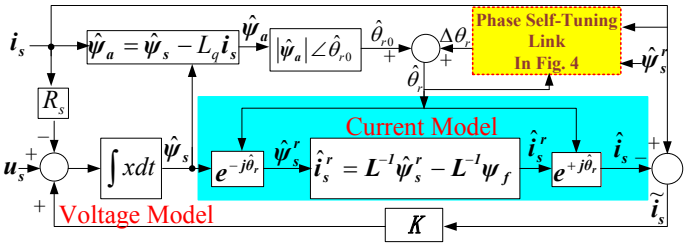

Fig. 5 The proposed stator flux observer based on active flux concept with phase self-tuning.

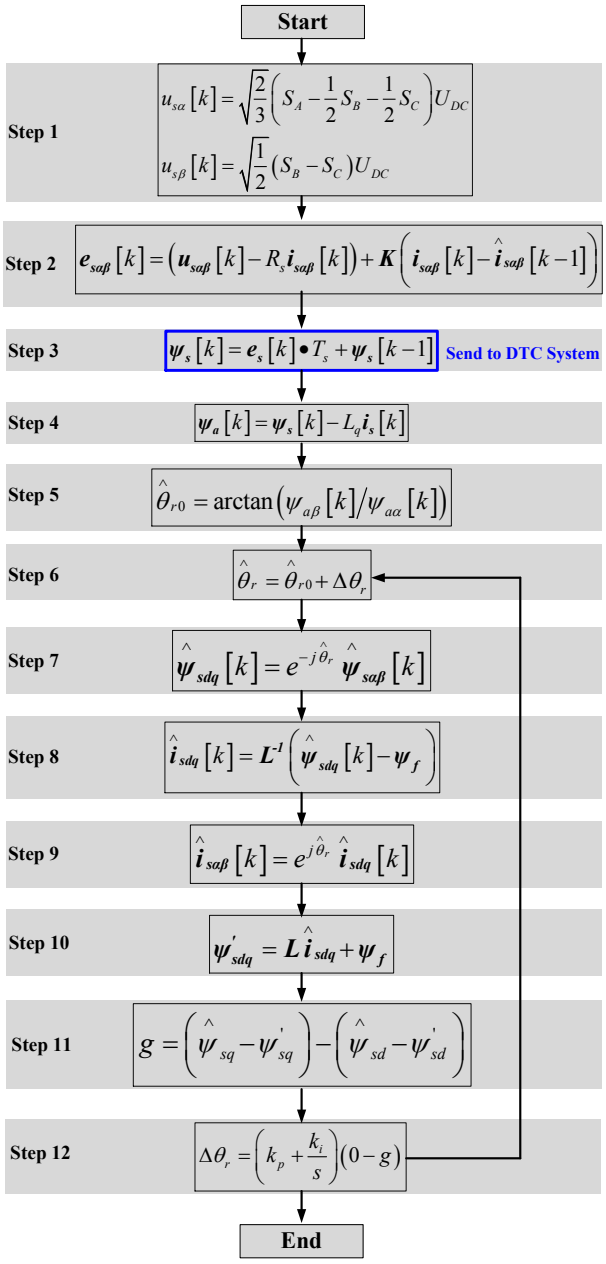

Fig. 6 Program flowchart of the proposed stator flux observer.

angle $\hat{\theta}_{r0}$ is obtained according to the active flux concept. Then, the variable g is sent to a PI regulator to output the value of the angle increment $\Delta\theta_r$. $\hat{\theta}_r$ is the observed rotor position angle after adjusting, its expression is $\hat{\theta}_r = \hat{\theta}_{r0} + \Delta\theta_r$. The proposed stator flux observer as shown in Fig. 5 not only shares the advantages of conventional stator flux observer based on active flux concept, but also overcomes its disadvantages. Hence, it is suitable for high-performance direct torque control drive occasions with strict requirements.

In addition, it is important to note that if the mismatch of motor parameters is serious to some extent, $\Delta\theta_r$ may be fall beyond $[-\pi/4, \pi/4]$ (although it is not easy to happen). In this case, it is difficult to achieve the desired control effect only by the proposed stator flux observer. In order to further improve its performance, motor parameter identification strategies, such as that in [26], should be combined with the proposed stator flux observer. However, it is not the focus of this paper. So, more detail introduction is not provided.

The program flow chart in Fig. 6 is provided to help describe the implementation of the proposed strategy. The concrete implementation steps are summarized as follows:

Step 1: Calculate the stator voltage $\boldsymbol{u}_{s\alpha\beta}[k]$ in stator static coordinate system according to switching combination and DC bus voltage U_{DC};

Step 2: Based on the observed stator current in previous control period $\hat{\boldsymbol{i}}_{s\alpha\beta}[k-1]$, the measured stator current $\boldsymbol{i}_{s\alpha\beta}[k]$ and the obtained stator voltage $\boldsymbol{u}_{s\alpha\beta}[k]$ in step 1, the back electromotive force (back-EMF) $\boldsymbol{e}_{s\alpha\beta}[k]$ can be calculated;

Step 3: Calculate stator flux $\boldsymbol{\psi}_{s\alpha\beta}[k]$ by integral of $\boldsymbol{e}_{s\alpha\beta}[k]$;

Step 4: Substitute the stator flux $\boldsymbol{\psi}_{s\alpha\beta}[k]$ and the actual stator current $\boldsymbol{i}_{s\alpha\beta}[k]$ into (8) to obtain the active flux vector $\boldsymbol{\psi}_{a\alpha\beta}[k]$;

Step 5: Substitute the active flux vector $\boldsymbol{\psi}_{a\alpha\beta}[k]$ into (9) to achieve the initial value of observed rotor position angle $\hat{\theta}_{r0}$;

Step 6: By adding the incremental of the rotor position angle $\Delta\theta_r$, which is the output of proposed phase self-tuning link, to the initial rotor position angle $\hat{\theta}_{r0}$, the rotor position angle after adjusting $\hat{\theta}_r$ can be achieved;

Step 7: Based on the $\hat{\theta}_r$ obtained in previous step, $\boldsymbol{\psi}_{s\alpha\beta}[k]$ can be transformed to d'-q' axes. Therefore, $\hat{\boldsymbol{\psi}}_{sdq}[k]$ can be obtained;

Step 8: Substitute $\hat{\boldsymbol{\psi}}_{sdq}[k]$ into (6) to obtain the observed stator current $\hat{\boldsymbol{i}}_{sdq}[k]$ in current control period;

Step 9: Transform $\hat{\boldsymbol{i}}_{sdq}[k]$ to the stator static coordinate system, then $\hat{\boldsymbol{i}}_{s\alpha\beta}[k]$ is obtained. Remarkably, this value is stored and utilized in step 2 of next control period;

Step 10: Based on $\hat{\boldsymbol{i}}_{sdq}[k]$ obtained in step 8, the observed values of stator flux $\boldsymbol{\psi}'_{sdq}[k]$ is calculated according to (31) and (32);

This article has been accepted for publication in a future issue of this journal, but has not been fully edited. Content may change prior to final publication. Citation information: DOI 10.1109/TPEL.2019.2952668, IEEE Transactions on Power Electronics

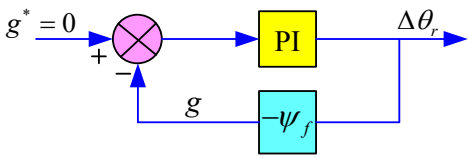

Fig. 7 The simplified control diagram of the proposed phase self-tuning link.

Step 11: Substitute $\hat{\psi}_{sdq}[k]$ obtained in step 7 and $\psi'_{sdq}[k]$ obtained in step 10 into formula (33) to achieve the variable g;

Step 12: Send the difference between 0 and g to the PI regulator. Its output value is as the incremental of the rotor position angle $\Delta\theta_r$, which can be used to adjust the initial value of rotor position angle in step 6.

It is noteworthy that the output values in step 3 are as the stator flux vectors utilized in the closed-loop DTC system.

C. Value Range of PI Parameters in the Proposed Phase Self-Tuning Link

The expression of the variable g shown in formula (34) can be further deduced as below.

$$g = -\psi_f\left(\sin\Delta\theta_r - \cos\Delta\theta_r + 1\right) \tag{35}$$

In the case that the observed error of rotor position angle is small enough, the following expressions can be obtained:

$$\sin\Delta\theta_r \approx \Delta\theta_r \tag{36}$$

$$\cos\Delta\theta_r \approx 1 \tag{37}$$

Substitute the expressions of (36) and (37) into the formula (35), the variable g can be rewritten as :

$$g \approx -\psi_f \Delta\theta_r \tag{38}$$

According to the deduction in (35)-(38), the control diagram of proposed phase self-tuning link can be simplified as shown in Fig. 7.

The closed-loop transfer function of Fig. 7 can be deduced as follows:

$$\frac{g}{g^*} \approx \frac{\left(k_p + \frac{k_i}{s}\right)\left(-\psi_f\right)}{1 + \left(k_p + \frac{k_i}{s}\right)\left(-\psi_f\right)} = \frac{-\psi_f\left(sk_p + k_i\right)}{\left(1 - k_p\psi_f\right)s - k_i\psi_f} \tag{39}$$

The pole of the closed-loop transfer function is calculated as shown in (40).

$$s = \frac{k_i\psi_f}{\left(1 - k_p\psi_f\right)} \tag{40}$$

In order to guarantee the stability of the proposed phase self-tuning link, the pole should be in the left-half plane. Therefore, one of the following conditions should be satisfied: 1) $k_i < 0$ and $k_p < 0$; 2) $k_i < 0$ and $0 < k_p < 1/\psi_f$; 3) $k_i > 0$ and $k_p > 1/\psi_f$. In this paper, k_p and k_i are respectively -50 and -1000. Consider that the limitation of the PI regulator should fall in the region of $[-\pi/4, \pi/4]$, it is set as 0.4 rad.

D. DTC System of PMSM Based on The Proposed Stator Flux Observer

The proposed stator flux observer with phase self-tuning is applied to the closed-loop DTC system for PMSM. The control diagram is shown in Fig. 8, where the part highlighted by red color is the proposed stator flux observer. The electromagnetic torque is the multiplication cross results of stator flux vector and stator current vector. The observed speed calculated according to (10) is utilized in the speed loop, thus the position sensorless can be realized above a certain speed. The output of the speed loop is the command value of electromagnetic torque.

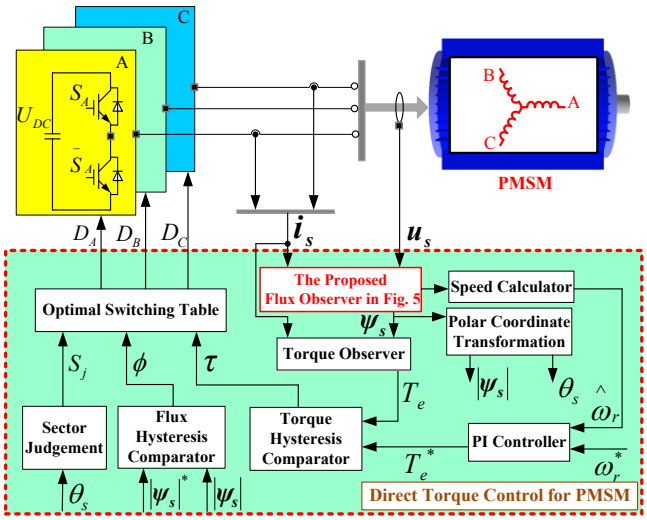

Fig. 8 Control diagram of direct torque control for PMSM.

As shown in Fig. 8, the closed loops of electromagnetic torque and stator flux are adopted in the inner loops, and two hysteresis comparators are utilized. $D_A \sim D_C$ are the switching states of three phases. S_j is the sector of stator flux, ϕ and τ are the output values of stator flux hysteresis comparator and electromagnetic torque hysteresis comparator, respectively.

An appropriate switching combination is obtained by looking up the optimal switching table according to S_j, ϕ and τ. Then, the electromagnetic torque and stator flux can be controlled simultaneously by applying the selected switching combination to the inverter. The optimal switching table in Fig. 8 has been introduced in many published literatures, such as [10]. Hence, no further description is provided in this paper.

V. Experimental Research

A. Experimental Platform and Parameters

The experimental platform is shown in Fig. 9. The parameters of three-phase PMSM utilized in this paper are listed in Tab. I. TI TMS320F28335 DSP is selected as the control chip, another permanent magnet synchronous generator (PMSG) with the same power works as the load. The sampling frequency is 20KHz. In this paper, the waveforms of phase currents are directly measured by current probes, and the waveforms of other variables are obtained by digital to analog conversion (DAC). Both of the hysteresis comparator bands of electromagnetic torque and stator flux are set as zero.

B. Experimental Research on the Robustness to Motor Parameters Variation

In order to research the robustness of the proposed stator flux observer, the stator flux observer based on current model as

This article has been accepted for publication in a future issue of this journal, but has not been fully edited. Content may change prior to final publication. Citation information: DOI 10.1109/TPEL.2019.2952668, IEEE Transactions on Power Electronics

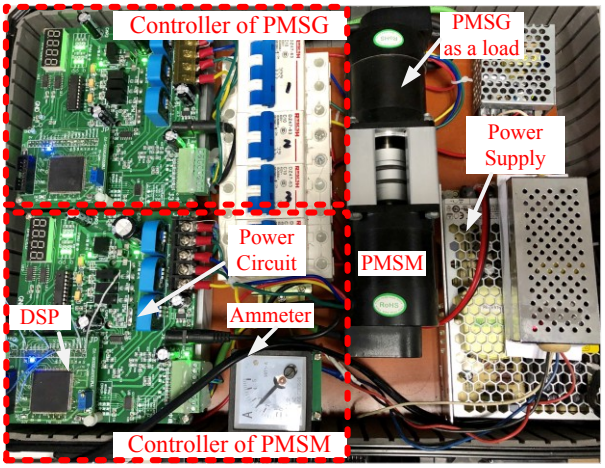

Fig. 9. Experimental platform.

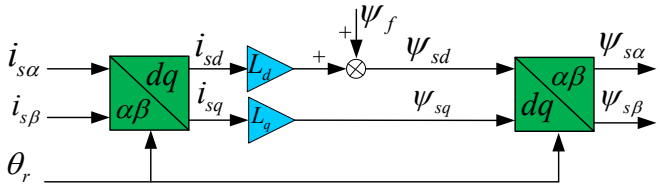

Fig. 10 The stator flux observer based on current model.

TABLE I
PARAMETERS OF THREE-PHASE PMSM

d-axis inductance	L_d	1.2385mH
q-axis inductance	L_q	1.6385mH
Number of pole pairs	n_p	2
Stator resistance	R_s	0.31Ω
Rated power	P	70w
Rated speed	n	3000r/min
DC bus voltage	U_{DC}	24V
Rated torque	Te	0.22N.m
Permanent magnet flux amplitude	ψ_f	0.01428Wb

shown in Fig. 10 is utilized in the closed-loop DTC system. It should be pointed out that the stator flux observer shown in Fig. 10 has two functions in this paper: 1) In Section V.B, it is utilized in the closed-loop DTC system. In the meanwhile, the conventional stator flux observer and the proposed stator flux observer are compared by open-loop mode; 2) In Section V.C and Section V.D, the conventional and the proposed stator flux observers are operated in closed-loop mode. In this case, the values obtained by Fig. 10 are considered as the actual values, which are used to compare with the observed values.

Experimental research on the robustness to motor parameter variation has been done at rated condition. The motor parameters are reset in the program to simulate the mismatch conditions. Remarkably, only the motor parameters used in the stator flux observers are changed. Figs. 11-14 are the experimental results with rated load at rated speed 3000rpm.

Figs. 11(a)-(c) are the experimental results when stator resistance is increased by 40%. The experimental results in Fig. 11(a) show that the observed error of the conventional stator flux observer is relatively large, whose maximum value is 0.0024Wb. However, the observed error of stator flux is greatly reduced after adding the proposed phase self-tuning method. The maximum observed error of the proposed stator flux observer is 0.0012Wb. As shown in Fig. 11(b), the observed

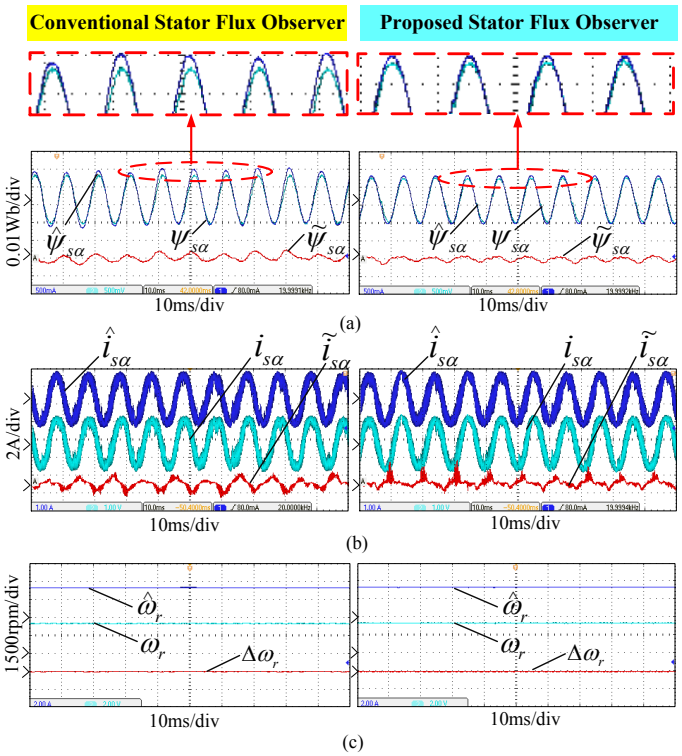

Fig. 11. Experimental results when stator resistance is increased by 40% for the basic stator flux observer and the proposed stator flux observer at 3000rpm. (a) The actual stator flux and the observed stator flux. (b) The actual stator current and the observed stator current.(c)The actual speed and the observed speed.

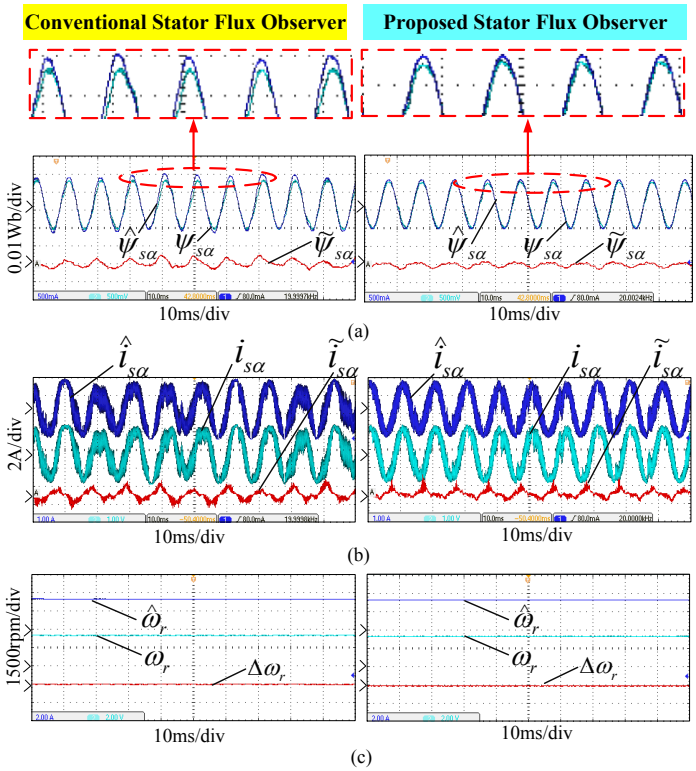

Fig. 12. Experimental results when *d*-axis inductance is decreased by 30% for the basic stator flux observer and the proposed stator flux observer at 3000rpm. (a) The actual stator flux and the observed stator flux. (b) The actual stator current and the observed stator current. (c)The actual speed and the observed speed.

stator currents can both track the actual currents well for these

This article has been accepted for publication in a future issue of this journal, but has not been fully edited. Content may change prior to final publication. Citation information: DOI 10.1109/TPEL.2019.2952668, IEEE Transactions on Power Electronics

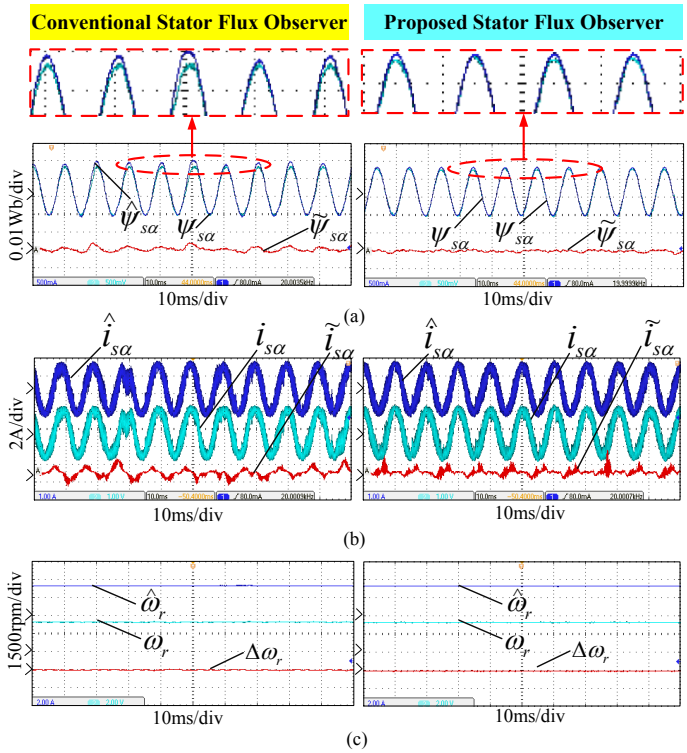

Fig. 13. Experimental results when q-axis inductance is decreased by 30% for the basic stator flux observer and the proposed stator flux observer at 3000rpm. (a) The actual stator flux and the observed stator flux. (b) The actual stator current and the observed stator current. (c)The actual speed and the observed speed.

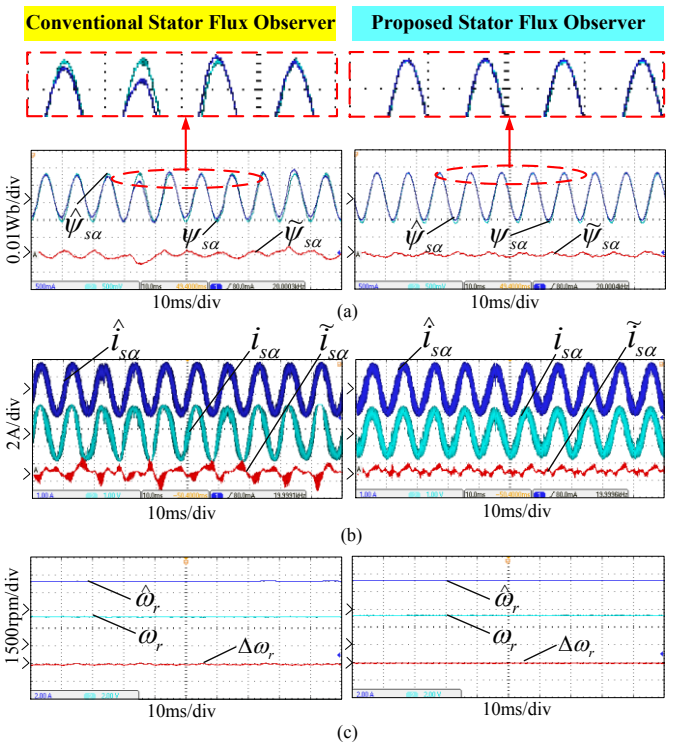

Fig. 14. Experimental results when permanent magnet flux is decreased by 20% for the basic stator flux observer and the proposed stator flux observer at 3000rpm. (a) The actual stator flux and the observed stator flux. (b) The actual stator current and the observed stator current. (c)The actual speed and the observed speed.

two stator observers. However, the observed error of the stator current is smaller in the proposed stator flux observer. As can be seen in Figs. 11(c), the observed error of speed are relatively small for these two observers. At rated condition, their maximum values are 12rpm and 9rpm, respectively. The experimental results in Fig. 11 show that the proposed stator flux observer has stronger robustness and higher accuracy under the condition of stator resistance variation.

Figs. 12(a)-(c) are the experimental results when d-axis inductance is decreased by 30%. Compared with the experimental result of the conventional stator flux observer, the maximum observed error of stator flux is reduced from 0.0025Wb to 0.0012Wb in the proposed stator flux observer. As shown in Fig. 12(b), the maximum observed errors of stator current in the conventional stator flux observer and the proposed stator flux observer are 0.48A and 0.42A, respectively. Compared with the conventional stator flux observer, the observed error of stator current is reduced greatly in the proposed stator flux observer. Furthermore, both of these two stator flux observers have high observed accuracy of speed as shown in Fig. 12(c), whose maximum observed errors are respectively 13rpm and 11rpm. The observed accuracy and robustness is improved in the proposed stator flux observer thanks to the proposed phase self-tuning link. The experimental results in Fig. 12 show that the robustness and accuracy of the proposed stator flux observer is obviously better than that of the conventional stator flux observer under the condition of d-axis inductance variation.

Figs. 13(a)-(c) are the experimental results when q-axis inductance is decreased by 30%. As shown in Fig. 13(a), both of the observed values of stator flux can track the actual values well under the condition of q-axis inductance variation. However, the accuracy of the proposed stator flux observer is higher. The maximum observed errors of the stator flux are respectively 0.0023Wb and 0.0009Wb in the conventional stator flux observer and the proposed stator flux observer. As shown in Fig. 13(b), the maximum observed error of stator current is reduced from 0.54A to 0.37A after the phase self-tuning link is added. As shown in Fig. 13(c), both of the observed errors of speed are relatively small in the conventional and the proposed stator flux observers. The experimental results in Figs. 13(a)-(c) verify the effectiveness of the proposed phase self-tuning link. Consequently, the proposed stator flux observer with phase self-tuning has stronger robustness and higher accuracy under the condition of q-axis inductance variation.

When the permanent magnet flux is reduced by 20%, the experimental results are shown in Figs. 14(a)-(c). The observed error of stator flux are 0.0026Wb and 0.0011Wb in the conventional and the proposed stator flux observers, respectively. As shown in Fig. 14(a), the observed error of stator flux is relatively large in the conventional stator flux observer. However, the observed stator flux can track the actual value well in the proposed stator flux observer even under the permanent magnet flux vary condition. The experimental results in Fig. 14(b) show that stator current in the proposed stator flux observer is better than that in the conventional stator flux observer. Their maximum observed errors of stator current are 0.53A and 0.38A, respectively. As shown in Fig. 14(c), the maximum observed error of speed are respectively 20rpm and

This article has been accepted for publication in a future issue of this journal, but has not been fully edited. Content may change prior to final publication. Citation information: DOI 10.1109/TPEL.2019.2952668, IEEE Transactions on Power Electronics

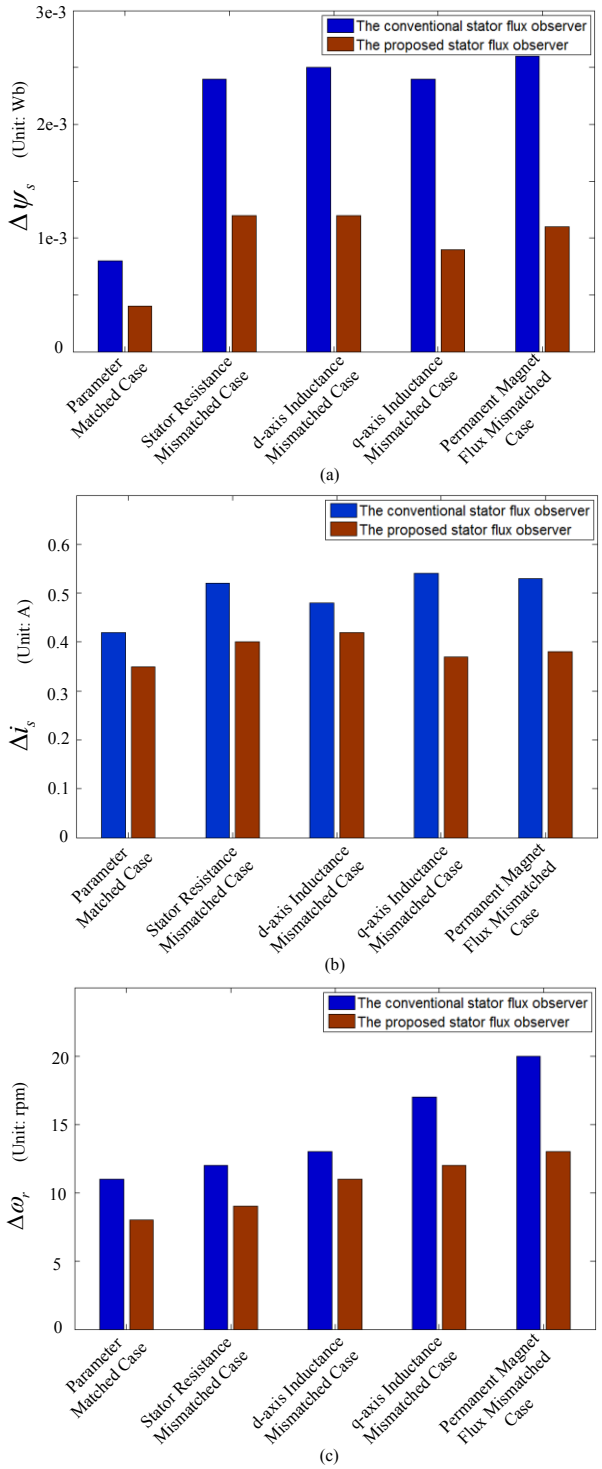

Fig. 15.Steady-state experimental results with rated load at rated speed 3000rpm (a) The maximum observed error of stator flux. (b) The maximum observed error of stator current. (c)The maximum observed error of speed.

13rpm for these two stator flux observers. The experimental results in Figs. 14(a)-(c) show that the robustness and accuracy of the proposed stator flux observer is improved under the condition of permanent magnet flux variation.

The experimental results in Figs. 11-14 can be summarized as shown in Fig. 15. As can be seen, the performance of the proposed stator flux observer is superior to the conventional stator flux observer under the conditions of parameters matched and parameters mismatched.

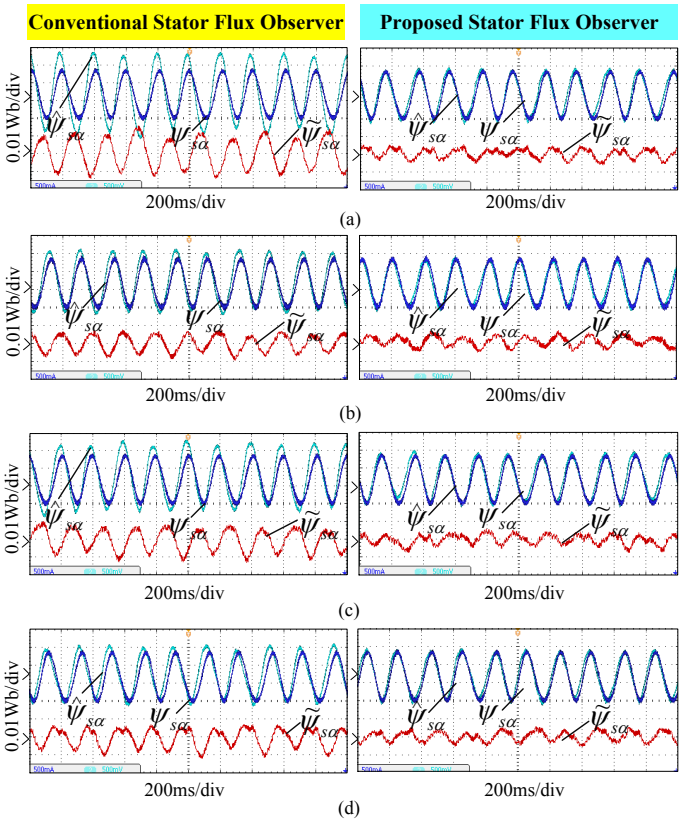

Fig. 16. Robust experimental results with rate load at low speed (150rpm). (a) The stator resistance is increased by 40%. (b) The *d*-axis inductance is decreased by 30%. (c) The *q*-axis inductance is decreased by 30%. (d) The permanent magnet flux is decreased by 20%.

In order to research the performance of the proposed stator flux observer at low speed, several experiments have been done. Figs. 16(a)-(d) are the robust experimental results with rated load at 150rpm. Compared with the experimental results in Figs. 11-14, the observed accuracy of stator flux is reduced for these two stator flux observers. However, the variation of the proposed stator flux observer is relatively small. In addition, as shown in Fig. 16, the proposed stator flux observer has obviously higher accuracy than the conventional stator flux observer under the motor parameters mismatched conditions. The experimental results in Figs. 16(a)-(d) verify that the proposed stator flux observer is effective at low speed.

C. Steady-State Experimental Research

In order to research the steady-state performance, the proposed stator flux observer with phase self-tuning is utilized in the closed loop system of DTC. Figs. 17 and 18 are the experimental results with rated load at rated speed 3000rpm of the conventional stator flux observer and the proposed stator flux observer, respectively.

As shown in Fig. 17(a), the actual electromagnetic torque can track the command electromagnetic torque very well. Both of their average value are 0.22N.m. Fig. 17(b) is the phase current with the amplitude of 3.4A. The results in Fig. 17(c) show that the observed stator flux is almost coincide with the actual one, whose maximum observed error is 0.0008Wb. In addition, as can be seen, the steady-state performance of closed-loop DTC system in Figs. 18(a)-(c) is better than those in Figs. 17(a)-(c).

This article has been accepted for publication in a future issue of this journal, but has not been fully edited. Content may change prior to final publication. Citation information: DOI 10.1109/TPEL.2019.2952668, IEEE Transactions on Power Electronics

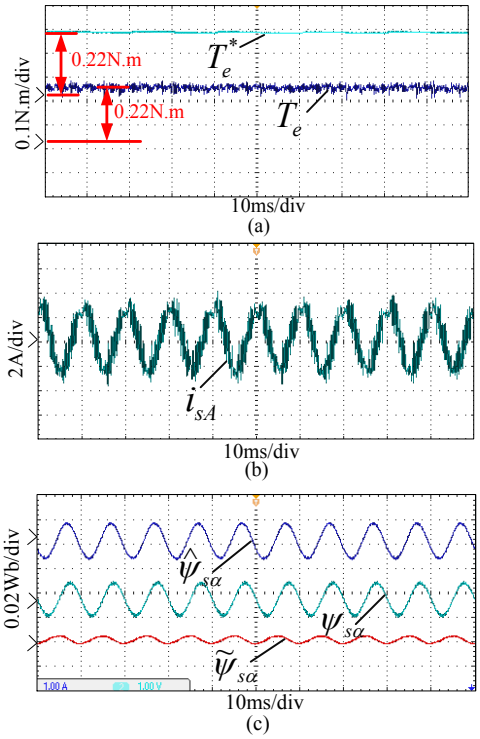

Fig.17. Steady-state experimental results of closed-loop DTC system based on the conventional stator flux observer. (a) The command value and the actual value of electromagnetic torque. (b) Phase current. (c) The observed and the actual value of stator flux.

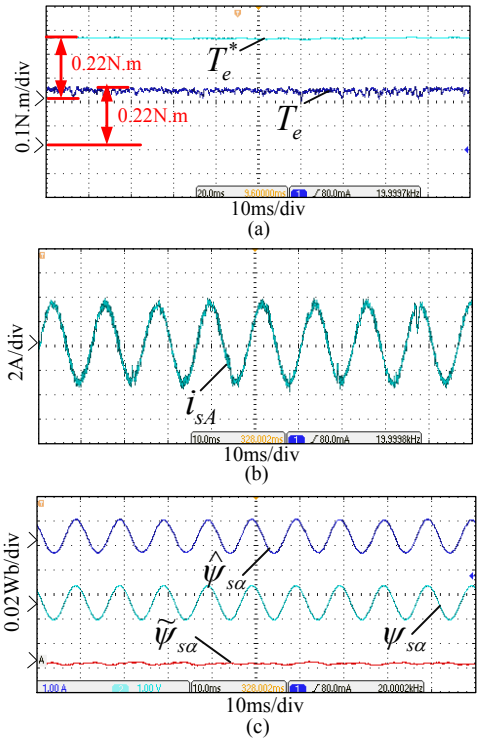

Fig.18. Steady-state experimental results of closed-loop DTC system based on the proposed stator flux observer. (a) The command value and the actual value of electromagnetic torque. (b) Phase current. (c) The observed and the actual value of stator flux.

This is for the reason that the proposed stator flux observer has higher accuracy. Then, the calculation of stator flux and

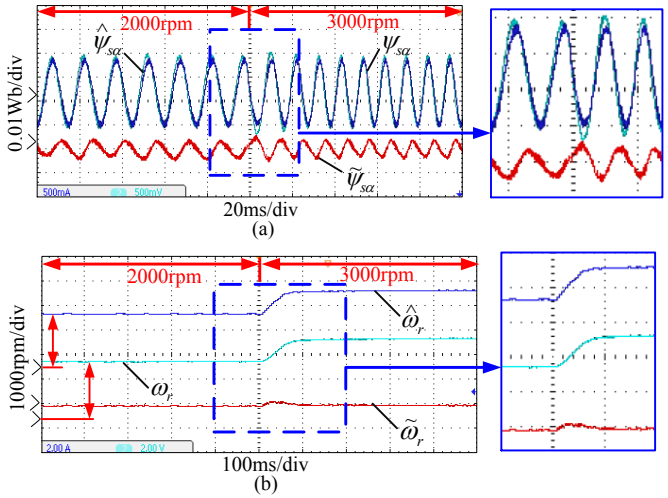

Fig.19. Speed step experiments of the closed-loop DTC system based on the conventional stator flux observer. (a) Stator flux. (b) Speed.

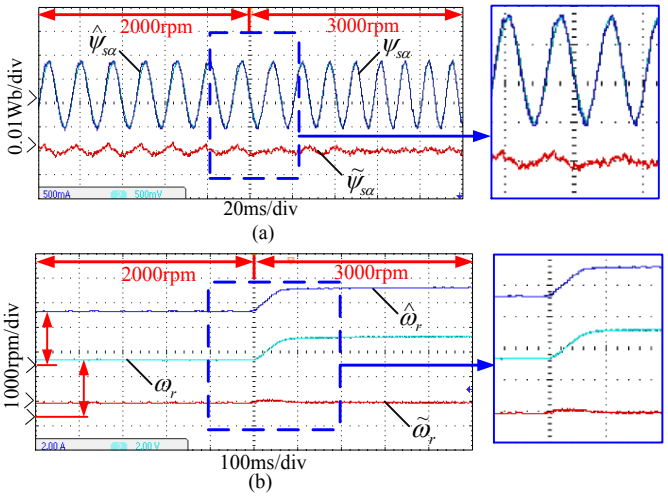

Fig.20. Speed step experiments of the closed-loop DTC system based on the proposed stator flux observer. (a) Stator flux. (b) Speed.

electromagnetic torque are closer to their actual values. The experimental results in Figs. 17 and 18 show that the steady-state performance of the closed-loop DTC system based on the proposed stator flux observer is superior to that based on the conventional stator flux observer.

D. Dynamic Experimental Research

Figs. 19 and 20 are the speed step experiments of the conventional stator flux observer and the proposed stator flux observer, respectively. In Figs. 19 and 20, the speed steps from 2000rpm to 3000rpm under no load condition. The experimental results show that the dynamic response is rapid in both Figs. 19 and 20. However, the observed errors in Figs. 20(a) and (b) are smaller than those in Figs. 19(a) and (b). Compared with the experimental results in Fig. 20, the observed errors of stator flux and speed in Fig. 19 are increased obviously during the dynamic process. This is because the observed rotor position cannot track its actual value well during this process. Then, the observed value of stator flux would be affected. However, this phenomenon is avoided in Fig. 20 for the reason that the proposed phase self-tuning link can make

This article has been accepted for publication in a future issue of this journal, but has not been fully edited. Content may change prior to final publication. Citation information: DOI 10.1109/TPEL.2019.2952668, IEEE Transactions on Power Electronics

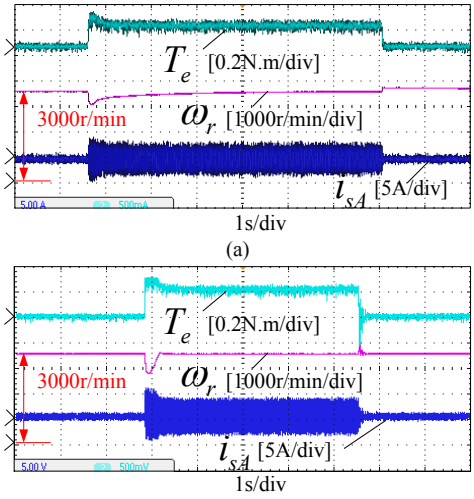

Fig.21. Load step experiments. (a) DTC based on the conventional stator flux observer. (b) DTC based on the proposed stator flux observer.

the observed coordinate system converge to actual coordinate system rapidly.

Figs. 21(a) and (b) are the load step experimental results of the DTC based on the conventional stator flux observer and the DTC based on the proposed stator flux observer, respectively. The load steps from no load to rate load at 3000rpm, then it is reduced from rated load to no load. The experimental results in Figs. 21(a) and (b) show that the dynamic response of the DTC system based on the proposed stator flux observer is as rapid as the DTC system based on the conventional stator flux observer.

VI. Conclusion

In this paper, a stator flux observer with phase self-tuning is proposed as an improved version of the conventional stator flux observer based on active flux concept. The contributions of this paper include:

1) The conventional stator flux observer based on active flux concept is introduced briefly, and the main reasons caused its weak robustness to motor parameters variation are analyzed;

2) According to the analysis results above, an improved version of stator flux observer with phase self-tuning is proposed to overcome the shortcomings of the conventional stator flux observer. Thanks to the proposed phase self-tuning link, the observed rotor synchronous coordinate system can converge to the actual coordinate system even under motor parameters mismatched conditions. Therefore, the robustness and accuracy of the stator flux observer can be enhanced;

3) The stability of the proposed phase self-tuning link is studied. Accordingly, a value range of PI parameters can be determined easily.

The performances of the conventional stator flux observer based on active flux concept and the proposed stator flux observer are compared by experimental research. The experimental results show that the proposed stator flux observer has stronger robustness to the variation of motor parameters, such as the stator resistance, *d*-axis inductance, *q*-axis inductance and permanent magnet flux, *et al*. Moreover, the proposed stator flux observer is applied to the DTC closed-loop system for PMSM, the excellent steady-state performance and rapid dynamic response can be obtained in this drive system.

References

[1] G. Liu, L. Chen, W. Zhao, Y. Jiang and L. Qu, "Internal model control of permanent magnet synchronous motor using support vector machine generalized inverse," *IEEE Trans. Ind. Inf.*, vol. 9, no. 2, pp. 890-898, May. 2013.

[2] M. A. M. Cheema, J. E. Fletcher, D. Xiao and M. F. Rahman, "A direct thrust control scheme for linear permanent magnet synchronous motor based on online duty ratio control," *IEEE Trans. Power Electron.*, vol. 31, no. 6, pp. 4416-4428, Jun. 2016.

[3] C. Lai, G. Feng, K. Mukherjee, J. Tjong and N. C. Kar, "Maximum torque per ampere control for IPMSM using gradient descent algorithm based on measured speed harmonics," *IEEE Trans. Ind. Inf.*, vol. 14, no. 4, pp. 1424-1435, Apr. 2018.

[4] K. Gulez, A. A. Adam and H. Pastaci, "Torque ripple and EMI noise minimization in PMSM using active filter topology and field-oriented control," *IEEE Trans. Ind. Electron.*, vol. 55, no. 1, pp. 251-257, Jan. 2018.

[5] J. Lara, J. Xu and A. Chandra, "Effects of rotor position error in the performance of field-oriented-controlled PMSM drives for electric vehicle traction applications," *IEEE Trans. Ind. Electron.*, vol.63, no. 8, pp. 4738-4751, Aug. 2016.

[6] M. Konghirun and L. Xu, "A fast transient-current control strategy in sensorless vector-controlled permanent magnet synchronous motor," *IEEE Trans. Power Electron.*, vol. 21, no. 5, pp. 1508-1512, Sep. 2006.

[7] L. Zhong, M. F. Rahman, Y. Hu and K. W. Lim, "Analysis of direct torque control in permanent magnet synchronous motor drives," *IEEE Trans. Power Electron.*, vol.12, no. 3, pp. 528-535, May. 1997.

[8] M. F. Rahman, L. Zhong, M. E. Haque and M. A. Rahman, "A direct torque-controlled interior permanent-magnet synchronous motor drive without a speed sensor," *IEEE Trans. Energy Conv.*, vol.18, no. 1, pp. 17-22, Mar. 2003.

[9] Z.Q. Zhu, Y. Ren and J. M. Liu, "Improved torque regulator to reduce steady-state error of torque response for direct torque control of permanent magnet synchronous machine drives," *IET Electr. Power Appl.*, vol.8, no. 3, pp. 108-116, Sep. 2014.

[10] X. Lin, W. Huang, W. Jiang, Y. Zhao, D. Dong and X. Wu, "Direct torque control for three-phase open-end winding PMSM with common DC bus based on duty ratio modulation," *IEEE Trans. Power Electron.*, doi.10.1109/TPEL.2019.2935295.

[11] Q. Liu and K. Hameyer, "Torque ripple minimization for direct torque control of PMSM with modified FCSMPC," *IEEE Trans. Ind. Appl.*, vol. 52, no. 6, pp. 602-612, Nov./Dec. 2016.

[12] F. Niu, K. Li and Y. Wang, "Direct torque control for permanent-magnet synchronous machines based on duty ratio modulation," *IEEE Trans. Ind. Electron.*, vol.62, no. 10, pp. 6160-6170, Oct. 2015.

[13] N. R. N. Idris and A. H. M. Yatim, "An improved stator flux estimation in steady-state operation for direct torque control of induction machines," *IEEE Trans. Ind. Appl.*, vol. 38, no. 1, pp. 110-116, Jan./Feb. 2002.

[14] J. Hu and B. Wu, "New integration algorithms for estimating motor flux over a wide speed range," *IEEE Trans. Power Electron.*, vol. 13, no. 5, pp. 969-977, Sep. 1998.

[15] H. Saberi, M. Sabahi, M. B. B. Sharifian and M. Feyzi, "Improved sensorless direct torque control method using adaptive flux observer," *IET Power Electron.*, vol. 7, no. 7, pp. 1676-1684, Jan. 2014.

[16] H. Kim, J. Son and J. Lee, "A high-speed sliding-mode observer for the sensorless speed control of a PMSM," *IEEE Trans. Ind. Electron.*, vol. 58, no. 9, pp. 4069-4077, Sep. 2011.

[17] W. Sun, Y. Yu, G. Wang, B. Li and D. Xu, "Design method of adaptive full order observer with or without estimated flux error in speed estimation algorithm," *IEEE Trans. Power Electron.*, vol. 31, no. 3, pp. 2609-2626, Mar. 2016.

[18] J. Qi, Y. Tian, Y. Gong and C. Zhu, "A sensorless initial rotor position estimation scheme and an extended Kalman filter observer for the direct torque controlled permanent magnet synchronous motor drive," *2008 International Conference on Electrical Machines and Systems (ICEMS)*, pp. 3945-3950, Oct. 2008.

[19] N. K. Quang, N. T. Hieu and Q. P. Ha, "FPGA-based sensorless PMSM speed control using reduced-order extended Kalman filters," *IEEE Trans. Ind. Electron.*, vol. 61, no. 12, pp. 6574-6582, Apr. 2014.

[20] I. Boldea, M. C. Paicu and G.-D. Andreescu, "Active flux concept for motion-sensorless unified AC drives," *IEEE Trans. Power Electron.*, vol. 23, no. 5, pp. 2612-2618, Sep. 2008.
[21] M. C. Paicu, I. Boldea, G.-D. Andreescu and F. Blaabjerg, "Very low speed performance of active flux based sensorless control: interior permanent magnet synchronous motor vector control versus direct torque and flux control," *IET Electr. Power Appl.*, vol.3, no. 6, pp. 551-561, Mar. 2009.
[22] G. H. B. Foo and M. F. Rahman, "Direct torque control of an IPM-synchronous motor drive at very low speed using a sliding-mode stator flux observer," *IEEE Trans. Power Electron.*, vol. 25, no. 4, pp. 933-942, Apr. 2010.
[23] D. Nguyen, R. Dutta, M. F. Rahman and J. E. Fletcher, "Performance of a sensorless controlled concentrated-wound interior permanent-magnet synchronous machine at low and zero speed," *IEEE Trans. Ind. Electron.*, vol. 63, no. 4, pp. 2016-2026, Apr. 2016.
[24] X. Lin, W. Huang, W. Jiang, Y. Zhao, D. Dong and S. Liu, "Position sensorless direct torque control for six-phase permanent magnet synchronous motor under two-phase open circuit," *IET Electr. Power Appl.*, doi: 10.1049/iet-epa.2018.5433.
[25] T. Sun, J. Wang and X. Chen, "Maximum torque per ampere (MTPA) control for interior permanent magnet synchronous machine drives based on virtual signal injection," *IEEE Trans. Power Electron.*, vol. 30, no. 9, pp. 5036-5045, Sep. 2015.
[26] S. Ichikawa, M. Tomita, S. Doki and S. Okuma, "Sensorless control of permanent-magnet synchronous motors using online parameter identification based on system identification theory," *IEEE Trans. Ind. Electron.*, vol. 53, no. 2, pp. 363-372, Apr. 2006.

Xiaogang Lin (S'18) was born in Quanzhou, Fujian Province, China in 1990. He received the B.S. degree in Electrical Engineering from Dalian Maritime University, Dalian, China, in 2012, and the Master's degrees from Fuzhou University, Fuzhou, China, in 2016. He is currently pursuing the Ph. D degree in Nanjing University of Aeronautics and Astronautics (NUAA), Nanjing, China. His main research interests are motor drive system.

Wenxin Huang (M'09) was born in Dongtai, Jiangsu Province, China, in 1966. He received the B.S. degree in the Southeast University, Nanjing, China, in 1988, and the Master's and Ph.D. degrees from Nanjing University of Aeronautics and Astronautics (NUAA), Nanjing, China, in 1994 and 2002, respectively.

In 2003, he joined the faculty of the College of Automation Engineering, NUAA, where he is currently a Professor. His research interests include stand-alone power systems, power electronics, design and control for electrical machine systems.

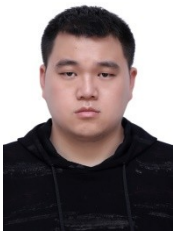

Wen Jiang (S'19) was born in Lianyungang, Jiangsu Province, China, in 1991. He received the B. S. degree in Electrical Engineering from Nanjing University of Aeronautics and Astronautics(NUAA), China, in 2014. He is currently working toward the Ph. D degree in Nanjing University of Aeronautics and Astronautics (NUAA), Nanjing, China. His main research interests are motor design and control.

Yong Zhao was born in Zhenjiang, Jiangsu Province, China, in 1991. He received the B. S. degree in Automation from Nanjing Institute of Technology (NJIT), Nanjing, China, in 2014. He is currently working toward the Ph. D degree in Nanjing University of Aeronautics and Astronautics (NUAA), Nanjing, China. His main research interests are motor design and control.

Shanfeng Zhu was born in Yancheng, Jiangsu Province, China, in 1995. He received the B. S. degree in Automation from Nanjing University of Aeronautics and Astronautics (NUAA), Nanjing, China, in 2017. He is currently working toward the Ph. D degree in NUAA, Nanjing, China. His main research interests are motor drive.